Freescale Semiconductor
Application Note

Document Number: AN3461
Rev. 6, 03/2013

Tilt Sensing Using a Three-Axis Accelerometer

by: Mark Pedley

1 Introduction

Accelerometers are sensitive to both linear acceleration and the local gravitational field. The former provides information on taps and other handset motions allowing the development of 'gesture' user interfaces while the latter provides information on the accelerometer orientation which allows a smartphone or tablet display to automatically switch between portrait and landscape settings.

This application note documents the mathematics of orientation determination using a three-axis accelerometer. The techniques are applicable to both digital accelerometers and, after signal digitization, to analog accelerometers. For convenience, it is assumed that the accelerometer is mounted in a smartphone or tablet but the arguments apply to any product with an embedded three-axis accelerometer.

Contents

freescale Xtrinsic

The following Freescale application notes cover related topics:

- AN4399 "High Precision Calibration of a Three Axis Accelerometer" describes how a product containing a consumer grade accelerometer can be re-calibrated after manufacture to achieve a high level of accuracy.
- AN4248 "Implementing a Tilt-Compensated eCompass using Accelerometer and Magnetometer Sensors" contains the mathematics and reference source code for a tilt-compensated eCompass where the accelerometer is used to correct for the magnetometer tilt from horizontal.
- AN4249 "Accuracy of Angle Estimation in eCompass and 3-D Pointer Applications" documents the effect of accelerometer sensor errors on roll and pitch angle accuracy and ultimately on the eCompass heading accuracy.

1.1 Key Words

Accelerometer, Tilt, Roll, Pitch, Portrait, Landscape.

1.2 Summary

1. Accelerometer sensors measure the difference between any linear acceleration in the accelerometer’s reference frame and the earth's gravitational field vector.
2. In the absence of linear acceleration, the accelerometer output is a measurement of the rotated gravitational field vector and can be used to determine the accelerometer pitch and roll orientation angles.
3. The orientation angles are dependent on the order in which the rotations are applied. The most common order is the aerospace sequence of yaw then pitch and finally a roll rotation.
4. Accelerometer sensors are insensitive to rotation about the earth's gravitational field vector. The equations for the roll and pitch angles therefore have mathematical instabilities when rotation axes happen to become aligned with gravity and point upwards or downwards. A workaround is presented to prevent this instability occurring.
5. Simple vector algebra expressions are derived for computing the tilt of the accelerometer from vertical or the rotation angle between any two accelerometer readings.
6. The most common application of accelerometers in consumer electronics is switching between portrait or landscape display modes. An algorithm is presented for controlling a tablet PC’s display orientation.

2 Accelerometer Output Under Gravity and Acceleration

Accelerometers are sensitive to the difference between the linear acceleration of the sensor and the local gravitational field. The data sheet for any accelerometer will denote the positive *x*, *y*, and *z* axes on the sensor package and, by convention, these are defined so that a linear acceleration aligned in the direction of these axes will give a positive accelerometer output.

A gravitational field component aligned along the same axes directions will, however, result in a negative reading on the accelerometer. This can be understood by looking at an electron microscope image of a MEMS accelerometer. The upper proof mass is suspended by the restoring springs. Both a gravitational field directed to the left and a linear acceleration of the package to the right will deflect the proof mass to the left.

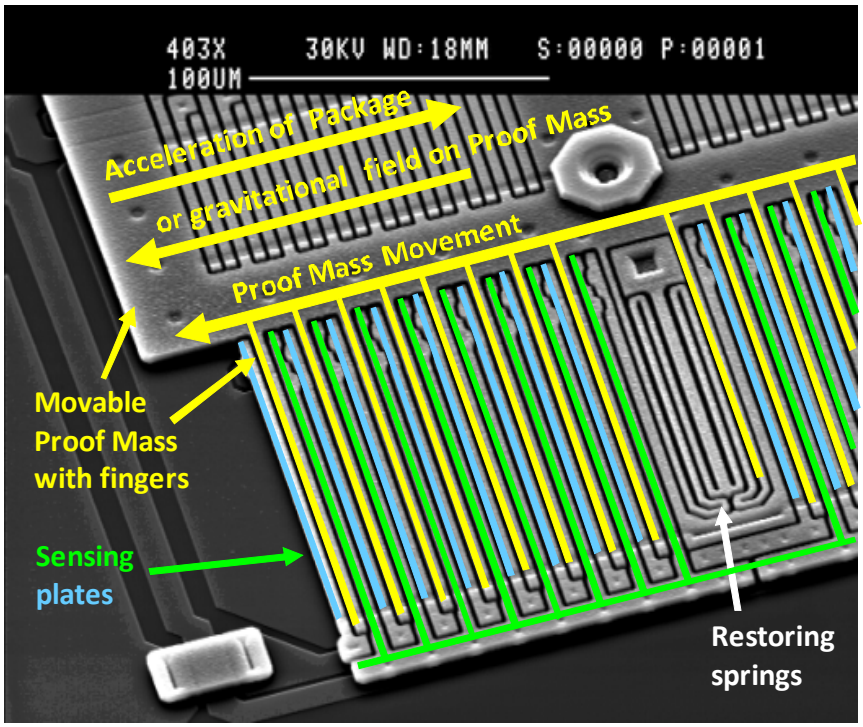

Figure 1. Electron Microscope Image of MEMS Accelerometer Proof Mass and Sensing Plates

The deflection of the proof mass is measured from the change in capacitance between the fingers of the proof mass and the sensing plates. A simplified transducer model and equivalent electrical circuit are shown in Figure 2. Circuitry internal to the accelerometer sensor converts the tiny capacitance to a voltage signal which, in digital accelerometers, is then digitized and output as a digital word over a serial bus.

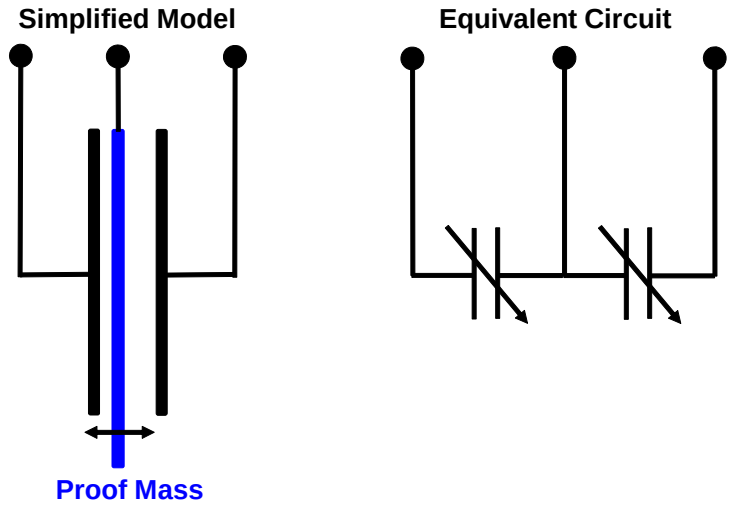

Figure 2. Simplified Transducer Model and Equivalent Electrical Circuit

The 'native' coordinate system of the accelerometer is not a convenient system to use when discussing the orientation of a consumer product, such as a smartphone, since the accelerometer can be mounted at any orientation on the circuit board which can, in turn, be mounted at an arbitrary angle in the final product. It is more sensible to use a coordinate system aligned with the smartphone product axes. Figure 3 shows the coordinate system which will be used in this document:

- The *x-axis* is aligned along the body axis of the smartphone
- The *z-axis* points downwards so that it is aligned with gravity when the smartphone is flat on a table
- The *y-axis* is aligned at right angles to both the *x* and *z* axes so that the three axes form a right handed coordinate system.

Changes in orientation are described by rotations in roll ϕ, pitch θ and yaw ψ about the *x*, *y* and *z* axes respectively.

Figure 3. Definition of Coordinate System and Rotation Axes

In addition, since this document is concerned with measuring orientation in the earth's gravitational field, the convention will be adopted that the accelerometer output is negated to give value +1g in any axis aligned with the earth's downward gravitational field.

With this assumption, a three-axis accelerometer mounted in a smartphone oriented in the earth's gravitational field $\boldsymbol{g}$ and undergoing linear acceleration $\boldsymbol{a}_r$ measured in the earth's reference frame *r*, will have output $\boldsymbol{G}_p$ given by:

$$\boldsymbol{G}_p = \begin{pmatrix} G_{px} \\ G_{py} \\ G_{pz} \end{pmatrix} = \boldsymbol{R}(\boldsymbol{g} - \boldsymbol{a}_r) \qquad \textit{Eqn. 1}$$

where $\boldsymbol{R}$ is the rotation matrix describing the orientation of the smartphone relative to the earth's coordinate frame.

It is further assumed that:

- The accelerometer has no linear acceleration $\boldsymbol{a}_r \approx 0$. This assumption is needed to solve Equation 1 for the rotation matrix $\boldsymbol{R}$ and, in consequence, any linear acceleration from handshake or other sources will introduce errors into the orientation estimate.
- The initial orientation of the smartphone is lying flat with the earth's gravitational field aligned with the smartphone *z-axis*:

With these additional assumptions, the smartphone accelerometer output $\boldsymbol{G}_p$ (measured in the native accelerometer units of *g*) is:

$$\boldsymbol{G}_p = \begin{pmatrix} G_{px} \\ G_{py} \\ G_{pz} \end{pmatrix} = \boldsymbol{R}\boldsymbol{g} = \boldsymbol{R}\begin{pmatrix} 0 \\ 0 \\ 1 \end{pmatrix} \qquad \textbf{Eqn. 2}$$

The next section introduces the components of the rotation matrix $\boldsymbol{R}$ and describes how to determine the roll and pitch angles from the accelerometer reading.

3 Pitch and Roll Estimation

The orientation of the smartphone can be defined by its roll, pitch and yaw rotations from an initial position. The roll, pitch and yaw rotation matrices, which transform a vector (such as the earth's gravitational field vector $\boldsymbol{g}$) under a rotation of the coordinate system of Figure 3 by angles ϕ in roll, θ in pitch and ψ in yaw about the *x*, *y* and *z* axes respectively, are:

$$\boldsymbol{R}_x(\phi) = \begin{pmatrix} 1 & 0 & 0 \\ 0 & \cos\phi & \sin\phi \\ 0 & -\sin\phi & \cos\phi \end{pmatrix} \qquad \textbf{Eqn. 3}$$

$$\boldsymbol{R}_y(\theta) = \begin{pmatrix} \cos\theta & 0 & -\sin\theta \\ 0 & 1 & 0 \\ \sin\theta & 0 & \cos\theta \end{pmatrix} \qquad \textbf{Eqn. 4}$$

$$\boldsymbol{R}_z(\psi) = \begin{pmatrix} \cos\psi & \sin\psi & 0 \\ -\sin\psi & \cos\psi & 0 \\ 0 & 0 & 1 \end{pmatrix} \qquad \textbf{Eqn. 5}$$

There are six possible orderings of these three rotation matrices and, in principle, all are equally valid. The rotation matrices do not, however, commute meaning that the composite rotation matrix $\boldsymbol{R}$ depends on the order in which the roll, pitch and yaw rotations are applied. It is instructive to compute the values of the six possible composite rotation matrices $\boldsymbol{R}$ and to determine their effect on the earth's gravitational field of 1g initially aligned downwards along the *z-axis*.

$$\boldsymbol{R}_{xyz}\begin{pmatrix}0\\0\\1\end{pmatrix} = \boldsymbol{R}_x(\phi)\boldsymbol{R}_y(\theta)\boldsymbol{R}_z(\psi)\begin{pmatrix}0\\0\\1\end{pmatrix} \quad \textit{Eqn. 6}$$

$$= \begin{pmatrix} \cos\theta\cos\psi & \cos\theta\sin\psi & -\sin\theta \\ \cos\psi\sin\theta\sin\phi - \cos\phi\sin\psi & \cos\phi\cos\psi + \sin\theta\sin\phi\sin\psi & \cos\theta\sin\phi \\ \cos\phi\cos\psi\sin\theta + \sin\phi\sin\psi & \cos\phi\sin\theta\sin\psi - \cos\psi\sin\phi & \cos\theta\cos\phi \end{pmatrix}\begin{pmatrix}0\\0\\1\end{pmatrix} \quad \textit{Eqn. 7}$$

$$= \begin{pmatrix} -\sin\theta \\ \cos\theta\sin\phi \\ \cos\theta\cos\phi \end{pmatrix} \quad \textit{Eqn. 8}$$

$$\boldsymbol{R}_{yxz}\begin{pmatrix}0\\0\\1\end{pmatrix} = \boldsymbol{R}_y(\theta)\boldsymbol{R}_x(\phi)\boldsymbol{R}_z(\psi)\begin{pmatrix}0\\0\\1\end{pmatrix} \quad \textit{Eqn. 9}$$

$$= \begin{pmatrix} \cos\psi\cos\theta - \sin\theta\sin\phi\sin\psi & \sin\psi\cos\theta + \sin\theta\sin\phi\cos\psi & -\sin\theta\cos\phi \\ -\cos\phi\sin\psi & \cos\phi\cos\psi & \sin\phi \\ \cos\theta\sin\phi\sin\psi + \sin\theta\cos\psi & -\cos\psi\cos\theta\sin\phi + \sin\psi\sin\theta & \cos\theta\cos\phi \end{pmatrix}\begin{pmatrix}0\\0\\1\end{pmatrix} \quad \textit{Eqn. 10}$$

$$= \begin{pmatrix} -\sin\theta\cos\phi \\ \sin\phi \\ \cos\theta\cos\phi \end{pmatrix} \quad \textit{Eqn. 11}$$

$$\boldsymbol{R}_{xzy}\begin{pmatrix}0\\0\\1\end{pmatrix} = \boldsymbol{R}_x(\phi)\boldsymbol{R}_z(\psi)\boldsymbol{R}_y(\theta)\begin{pmatrix}0\\0\\1\end{pmatrix} \quad \textit{Eqn. 12}$$

$$= \begin{pmatrix} \cos\theta\cos\psi & \sin\psi & -\cos\psi\sin\theta \\ -\cos\phi\cos\theta\sin\psi + \sin\phi\sin\theta & \cos\phi\cos\psi & \cos\theta\sin\phi + \cos\phi\sin\theta\sin\psi \\ \cos\theta\sin\psi\sin\phi + \cos\phi\sin\theta & -\cos\psi\sin\phi & \cos\theta\cos\phi - \sin\theta\sin\phi\sin\psi \end{pmatrix}\begin{pmatrix}0\\0\\1\end{pmatrix} \quad \textit{Eqn. 13}$$

$$= \begin{pmatrix} -\cos\psi\sin\theta \\ \cos\theta\sin\phi + \cos\phi\sin\psi\sin\theta \\ \cos\phi\cos\theta - \sin\theta\sin\phi\sin\psi \end{pmatrix} \quad \textit{Eqn. 14}$$

$$\boldsymbol{R}_{yzx}\begin{pmatrix} 0 \\ 0 \\ 1 \end{pmatrix} = \boldsymbol{R}_y(\theta)\boldsymbol{R}_z(\psi)\boldsymbol{R}_x(\phi)\begin{pmatrix} 0 \\ 0 \\ 1 \end{pmatrix} \quad \textit{Eqn. 15}$$

$$= \begin{pmatrix} \cos\psi\cos\theta & \cos\phi\cos\theta\sin\psi + \sin\theta\sin\phi & \cos\theta\sin\phi\sin\psi - \sin\theta\cos\phi \\ -\sin\psi & \cos\phi\cos\psi & \cos\psi\sin\phi \\ \cos\psi\sin\theta & -\cos\theta\sin\phi + \cos\phi\sin\psi\sin\theta & \cos\theta\cos\phi + \sin\theta\sin\phi\sin\psi \end{pmatrix}\begin{pmatrix} 0 \\ 0 \\ 1 \end{pmatrix} \quad \textit{Eqn. 16}$$

$$= \begin{pmatrix} \cos\theta\sin\phi\sin\psi - \cos\phi\sin\theta \\ \cos\psi\sin\phi \\ \cos\theta\cos\phi + \sin\theta\sin\phi\sin\psi \end{pmatrix} \quad \textit{Eqn. 17}$$

$$\boldsymbol{R}_{zxy}\begin{pmatrix} 0 \\ 0 \\ 1 \end{pmatrix} = \boldsymbol{R}_z(\psi)\boldsymbol{R}_x(\phi)\boldsymbol{R}_y(\theta)\begin{pmatrix} 0 \\ 0 \\ 1 \end{pmatrix} \quad \textit{Eqn. 18}$$

$$= \begin{pmatrix} \cos\psi\cos\theta + \sin\theta\sin\phi\sin\psi & \cos\phi\sin\psi & \cos\theta\sin\phi\sin\psi - \sin\theta\cos\psi \\ -\cos\theta\sin\psi + \cos\psi\sin\phi\sin\theta & \cos\phi\cos\psi & \cos\psi\cos\theta\sin\phi + \sin\theta\sin\psi \\ \cos\phi\sin\theta & -\sin\phi & \cos\theta\cos\phi \end{pmatrix}\begin{pmatrix} 0 \\ 0 \\ 1 \end{pmatrix} \quad \textit{Eqn. 19}$$

$$= \begin{pmatrix} \cos\theta\sin\phi\sin\psi - \cos\psi\sin\theta \\ \cos\psi\cos\theta\sin\phi + \sin\theta\sin\psi \\ \cos\theta\cos\phi \end{pmatrix} \quad \textit{Eqn. 20}$$

$$\boldsymbol{R}_{zyx}\begin{pmatrix}0\\0\\1\end{pmatrix} = \boldsymbol{R}_z(\psi)\boldsymbol{R}_y(\theta)\boldsymbol{R}_x(\phi)\begin{pmatrix}0\\0\\1\end{pmatrix} \quad \textit{Eqn. 21}$$

$$= \begin{pmatrix} \cos\psi\cos\theta & \cos\phi\sin\psi + \cos\psi\sin\phi\sin\theta & \sin\phi\sin\psi - \cos\phi\cos\psi\sin\theta \\ -\cos\theta\sin\psi & \cos\psi\cos\phi - \sin\theta\sin\phi\sin\psi & \cos\psi\sin\phi + \cos\phi\sin\psi\sin\theta \\ \sin\theta & -\cos\theta\sin\phi & \cos\theta\cos\phi \end{pmatrix}\begin{pmatrix}0\\0\\1\end{pmatrix} \quad \textit{Eqn. 22}$$

$$= \begin{pmatrix} \sin\phi\sin\psi - \cos\phi\cos\psi\sin\theta \\ \cos\psi\sin\phi + \cos\phi\sin\psi\sin\theta \\ \cos\theta\cos\phi \end{pmatrix} \quad \textit{Eqn. 23}$$

It can be readily seen from Equations 6 to 23 that the six composite rotation matrices and the six values of the measured gravitational vector are all different. A consequence is that roll, pitch and yaw rotation angles are meaningless without first defining the order in which these rotations are to be applied.

Four of these rotation sequences can be immediately rejected as being unsuitable for determining the smartphone orientation. The accelerometer output has three components but, since the vector magnitude must always equal 1g in the absence of linear acceleration, has just two degrees of freedom. The accelerometer vector lies on the surface of a sphere with radius 1g. It is not therefore possible to solve for three unique values of the roll ϕ, pitch θ and yaw ψ angles. The four rotation sequences in Equations 12 to 23 result in the accelerometer output being a function of all three rotation angles and cannot therefore be solved.

In contrast, the two rotation sequences in Equations 6 to 11 depend only on the roll ϕ and pitch θ angles and can be solved. The lack of any dependence on the yaw rotation angle ψ is easy to understand physically since the first rotation is in yaw ψ around the smartphone *z-axis* which is initially aligned with the gravitational field and pointing downwards. All accelerometers are completely insensitive to rotations about the gravitational field vector and cannot be used to determine such a rotation.

It is conventional therefore to select either the rotation sequence $\boldsymbol{R}_{xyz}$ of Equations 6 to 8 or the sequence $\boldsymbol{R}_{yxz}$ of Equations 9 to 11 to eliminate the yaw rotation ψ and allow solution for the roll ϕ and pitch θ angles. The unknown yaw angle ψ represents the smartphone rotation from north but its determination requires the addition of a magnetometer sensor to create an eCompass. Further details of the operation of a tilt-compensated eCompass can be found in application note AN4248.

Solving R_{xyz} (Equations 6 to 8) for the Pitch and Roll Angles

Equation 8 can be rewritten in the form of Equation 24 relating the roll ϕ and pitch θ angles to the normalized accelerometer reading $\boldsymbol{G}_p$:

$$\frac{\boldsymbol{G}_p}{\|\boldsymbol{G}_p\|} = \begin{pmatrix} -\sin\theta \\ \cos\theta\sin\phi \\ \cos\theta\cos\phi \end{pmatrix} \Rightarrow \frac{1}{\sqrt{G_{px}^{\ 2} + G_{py}^{\ 2} + G_{pz}^{\ 2}}} \begin{pmatrix} G_{px} \\ G_{py} \\ G_{pz} \end{pmatrix} = \begin{pmatrix} -\sin\theta \\ \cos\theta\sin\phi \\ \cos\theta\cos\phi \end{pmatrix} \quad \textbf{Eqn. 24}$$

Solving for the roll and pitch angles from Equation 24, and using the subscript *xyz* to denote that the roll and pitch angles are computed according to the rotation sequence $\boldsymbol{R}_{xyz}$, gives:

$$\tan\phi_{xyz} = \left(\frac{G_{py}}{G_{pz}}\right) \quad \textbf{Eqn. 25}$$

$$\tan\theta_{xyz} = \left(\frac{-G_{px}}{G_{py}\sin\phi + G_{pz}\cos\phi}\right) = \frac{-G_{px}}{\sqrt{G_{py}^{\ 2} + G_{pz}^{\ 2}}} \quad \textbf{Eqn. 26}$$

The rotation sequence $\boldsymbol{R}_{xyz}$ is widely used in the aerospace industry and is termed the 'aerospace rotation sequence'.

Solving R_{yxz} (Equations 9 to 11) for the Pitch and Roll angles

Equation 11 can be similarly solved for the roll and pitch angles from an arbitrary accelerometer reading $\boldsymbol{G}_p$:

$$\frac{\boldsymbol{G}_p}{\|\boldsymbol{G}_p\|} = \begin{pmatrix} -\sin\theta\cos\phi \\ \sin\phi \\ \cos\theta\cos\phi \end{pmatrix} \Rightarrow \frac{1}{\sqrt{G_{px}^{\ 2} + G_{py}^{\ 2} + G_{pz}^{\ 2}}} \begin{pmatrix} G_{px} \\ G_{py} \\ G_{pz} \end{pmatrix} = \begin{pmatrix} -\sin\theta\cos\phi \\ \sin\phi \\ \cos\theta\cos\phi \end{pmatrix} \quad \textbf{Eqn. 27}$$

Solving for the roll and pitch angles from Equation 27, and using the subscript *yxz* to denote that the angles are computed according to the rotation sequence $\boldsymbol{R}_{yxz}$, gives:

$$\tan\phi_{yxz} = \frac{G_{py}}{\sqrt{G_{px}^{\ 2} + G_{pz}^{\ 2}}} \quad \textbf{Eqn. 28}$$

$$\tan\theta_{yxz} = \left(\frac{-G_{px}}{G_{pz}}\right) \quad \textbf{Eqn. 29}$$

Equations 25 and 26 and Equations 28 and 29 therefore give different results for the roll and pitch angles from the same accelerometer reading. As mentioned earlier, this is a simple consequence of the fact that rotation matrices do not commute. The order of rotations is important and must always be specified when referring to specific orientation angles.

Eliminating Duplicate Solutions by Limiting the Roll and Pitch Ranges

The next complication to be addressed is that the expressions for the roll ϕ and pitch θ angles in Equations 25 and 26 and Equations 28 and 29 have an infinite number of solutions at multiples of 360°. Restricting the range of the roll and pitch angles to lie in the range -180° to 180° helps somewhat but the next paragraph shows that this still leads to two unique solutions for the roll and pitch angles.

Evaluating Equation 8 for pitch angle $\pi - \theta$ and roll angle $\phi + \pi$ and applying standard trigonometric identities shows that the accelerometer measurement is the same as that resulting from rotations θ and ϕ.

$$\begin{pmatrix} -sin(\pi - \theta) \\ cos(\pi - \theta)sin(\phi + \pi) \\ cos(\pi - \theta)cos(\phi + \pi) \end{pmatrix} = \begin{pmatrix} -sin\,\theta \\ cos\,\theta sin\,\phi \\ cos\,\theta cos\,\phi \end{pmatrix} \qquad \textit{Eqn. 30}$$

Similarly, evaluating Equation 11 for pitch angle $\theta + \pi$ and roll angle $\pi - \phi$ also shows that the accelerometer measurement is identical to that resulting from rotations θ and ϕ.

$$\begin{pmatrix} -sin(\theta + \pi)cos(\pi - \phi) \\ sin(\pi - \phi) \\ cos(\theta + \pi)cos(\pi - \phi) \end{pmatrix} = \begin{pmatrix} -sin\,\theta cos\,\phi \\ sin\,\phi \\ cos\,\theta cos\,\phi \end{pmatrix} \qquad \textit{Eqn. 31}$$

The solution is to restrict either the roll or the pitch angle (but not both) to lie between -90° and +90°. The convention used in the aerospace sequence is that the roll angle can range between -180° to +180° but the pitch angle is restricted to -90° to +90°. The convention used by Android™ smartphones and by Microsoft for its Windows 8 sensor platform is the reverse with the roll angle restricted between -90° and 90° but the pitch angle able to range between -180° and 180°. Whichever convention is used, the net result is to eliminate one of the two duplicate solutions and give a single solution except in the very specific orientations discussed later.

Worked Example 1

Determine the roll and pitch angles defining the orientation of the smartphone relative to the starting position with the smartphone flat on the table assuming the aerospace rotation sequence $\boldsymbol{R}_{xyz}$ for the smartphone accelerometer reading (in native units of g) below:

$$\boldsymbol{G}_p = \begin{pmatrix} 0.461105 \\ 0.082198 \\ -0.887432 \end{pmatrix}, |\boldsymbol{G}_p| = 1.006910 \qquad \textit{Eqn. 32}$$

Substituting the accelerometer reading into Equations 25 and 26 gives:

$$tan\,\phi_{xyz} = \frac{0.082198}{-0.887432} = -0.092625 \Rightarrow \phi_{xyz} = -5.2922° \text{or } 174.7081° \qquad \textit{Eqn. 33}$$

$$tan\,\theta_{xyz} = \frac{-0.461105}{\sqrt{0.082198^2 + 0.887432^2}} = -0.517380 \Rightarrow \theta_{xyz} = -27.3561° \qquad \textit{Eqn. 34}$$

The range of θ_{xyz} is -90° to 90° so there is a unique solution for θ_{xyz} in Equation 34. In Equation 33, however, ϕ_{xyz} can vary between -180° and 180° giving two possible solutions of -5.29° and 174.71°. Comparison with Equation 24 shows that the required solution which gives positive G_{py} and negative G_{pz} is 174.71°. In practice, this is not a problem for a software implementation provided that the ATAN2 function is used as ϕ_{xyz} = ATAN2(G_{py}, G_{pz}). The ATAN2 function automatically returns the angle (in radians) in the correct quadrant based on the signs of the two arguments.

Regions of Instability

The final complication is that both Equations 25 and 29 have a region where the calculation of the roll angle ϕ and pitch θ angle respectively become unstable.

The inverse tangent function for the aerospace rotation sequence in Equation 25 is mathematically defined for all values of G_{py} and G_{pz} with the one exception where both G_{py} and G_{pz} equal zero. This condition occurs when the smartphone is aligned with its *x-axis* pointing vertically upwards or downwards. Even if the smartphone is not exactly vertical, the inverse tangent calculation is dominated by accelerometer noise in the numerator and denominator of Equation 25 and produces an unstable and essentially random estimate of the roll angle. The physics is straightforward to understand: when the smartphone is vertical, the *x-axis* is vertical so that a rotation in roll is a rotation about the gravitational field vector which cannot be detected.

Similarly Equation 29 is defined for all values of G_{px} and G_{pz} with the exception where both G_{px} and G_{pz} are zero. This occurs when the smartphone is oriented on edge with the *y-axis* vertical and parallel to the earth's gravitational field vector so that any pitch θ rotation cannot be detected.

Equations 26 and 28, in contrast, are always defined and stable when the accelerometer is held in the earth's gravitational field. Applying the constraint that $G_{px}^2 + G_{py}^2 + G_{pz}^2 = 1g^2$ in Equations 26 and 28 shows that it is not possible for both numerator and denominator to be simultaneously zero and give an unstable angle estimate. When the numerator is zero, the denominator equals 1 and vice versa.

$$\tan\theta_{xyz} = \frac{-G_{px}}{\sqrt{1 - G_{px}^2}} \quad \text{(Caution: do not use)} \qquad \textit{Eqn. 35}$$

$$\tan\phi_{yxz} = \frac{G_{py}}{\sqrt{1 - G_{py}^2}} \quad \text{(Caution: do not use)} \qquad \textit{Eqn. 36}$$

Equations 35 and 36 should not, however, be used as alternatives to Equations 26 and 28 because any handshake, linear acceleration, sensor noise or simply using the accelerometer in a region of the world where the local gravitational field exceeds that at the original accelerometer calibration site can lead to G_{px} or G_{py} exceeding 1g and the square root and angle calculation having no real-valued solution.

There is no perfect solution to the problem of the roll and pitch angle singularities in Equations 25 and 29. One workaround, which is commonly used for the aerospace rotation sequence $\boldsymbol{R}_{xyz}$, is to use the numerically stable Equation 26 for calculation of the pitch angle θ but to modify Equation 25 for the roll angle ϕ by mixing a fraction μ of the square of the accelerometer *x-axis* reading G_{px}^2 into the denominator to prevent the denominator ever being zero. The resulting equations are:

$$\tan\theta_{xyz} = \frac{-G_{px}}{\sqrt{G_{py}^2 + G_{pz}^2}} \qquad \textit{Eqn. 37}$$

$$\tan\phi_{xyz} = \frac{G_{py}}{sign(G_{pz})\sqrt{G_{pz}^2 + \mu G_{px}^2}} \qquad \textit{Eqn. 38}$$

$sign(G_{pz})$ has a value +1 if G_{pz} is non-negative and -1 if G_{pz} is negative. This term is present to recover the loss sign of sign of G_{pz} when taking the square root. Obviously Equation 37 (which is identical to Equation 26) is mathematically correct for the aerospace sequence $\boldsymbol{R}_{xyz}$ and therefore always gives the correct pitch angle θ. Equation 38 for the roll angle ϕ is an approximation but has several characteristics that make it attractive:

- It is impossible for both numerator and denominator of Equation 38 to be simultaneously zero and give an undefined or unstable estimate of the roll angle.
- In the absence of any rotation in pitch θ, G_{px} equals zero and Equation 38 reduces to Equation 25 giving the correct roll angle ϕ.
- When the true roll angle is zero, G_{py} is also zero according to Equation 8. Equation 38 therefore correctly gives zero roll angle ϕ for all pitch angles θ.
- Equation 38 smoothly drives the roll angle ϕ to zero as the smartphone becomes oriented vertically upwards or downwards since G_{px}^2 approaches $1g^2$ and G_{py} and G_{pz} approach zero. This is reasonable behavior since the accelerometer reading is only dependent on the pitch angle θ when the smartphone is vertical and the roll angle is superfluous.

The roll angle error $\Delta\phi$ resulting from using the stable approximation of Equation 38 instead of the correct (but potentially unstable) Equation 25 is given by:

$$\Delta\phi = tan^{-1}\left(\frac{G_{py}}{\sqrt{G_{pz}^{\ 2} + \mu G_{px}^{\ 2}}}\right) - tan^{-1}\left(\frac{G_{py}}{G_{pz}}\right) \quad \textbf{Eqn. 39}$$

Using the trigonometric identity:

$$tan^{-1}a - tan^{-1}b = tan^{-1}\left(\frac{a-b}{1+ab}\right) \quad \textbf{Eqn. 40}$$

and Equation 8 allows Equation 39 to be simplified to:

$$\Delta\phi = tan^{-1}\left(\frac{G_{py}\left(G_{pz} - \sqrt{G_{pz}^{\ 2} + \mu G_{px}^{\ 2}}\right)}{G_{py}^{\ 2} + G_{pz}\sqrt{G_{pz}^{\ 2} + \mu G_{px}^{\ 2}}}\right) = tan^{-1}\left(\frac{sin\,\phi\left(cos\,\theta cos\,\phi - \sqrt{cos^2\theta cos^2\phi + \mu sin^2\theta}\right)}{cos\,\theta sin^2\phi + cos\,\phi\sqrt{cos^2\theta cos^2\phi + \mu sin^2\theta}}\right) \quad \textbf{Eqn. 41}$$

Figures 4 and 5 plot the absolute value of the resulting error $|\Delta\phi|$ in degrees computed from Equation 41 as a function of roll ϕ and pitch angles θ between -90° and 90° and with the contour mesh set to interval of 3° and μ equal to 0.01 and 0.1. It's clear that the stable approximation of Equation 38 gives an accurate estimate except at orientations approaching 90° where the roll angle error rises as its value is forced to zero for stability.

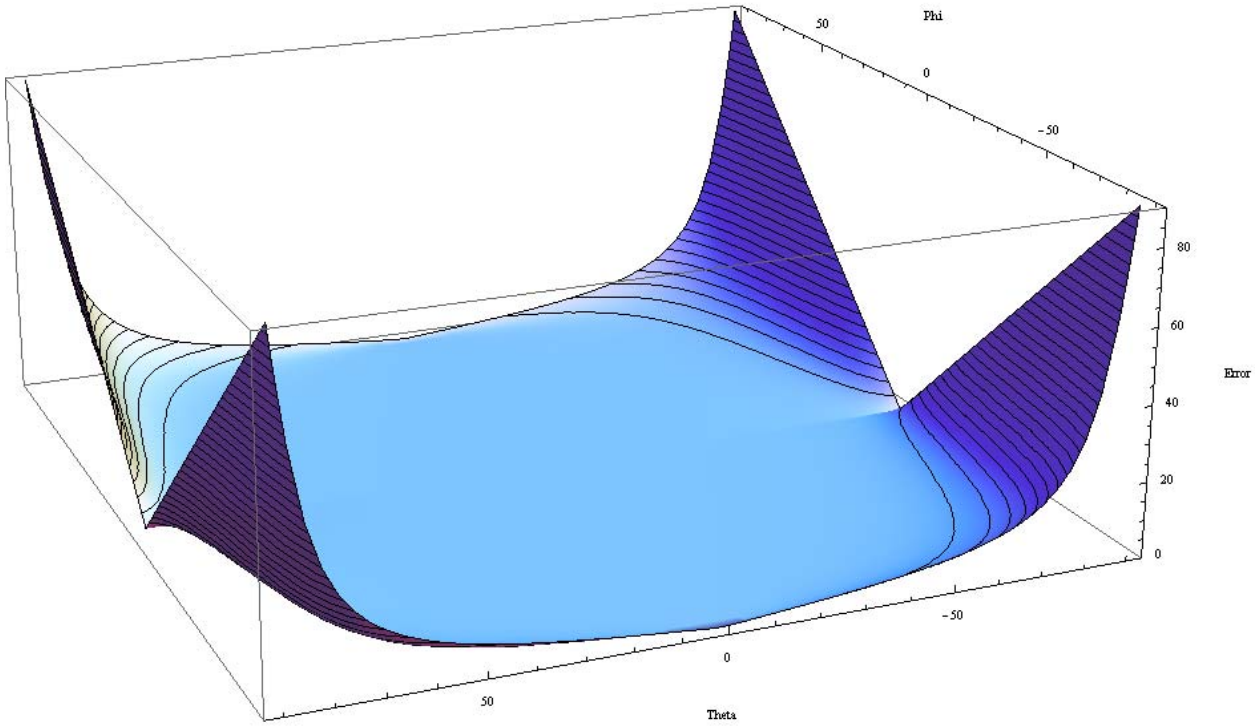

Figure 4. Roll Angle Error Surface $|\Delta\phi|$ for μ = 0.01

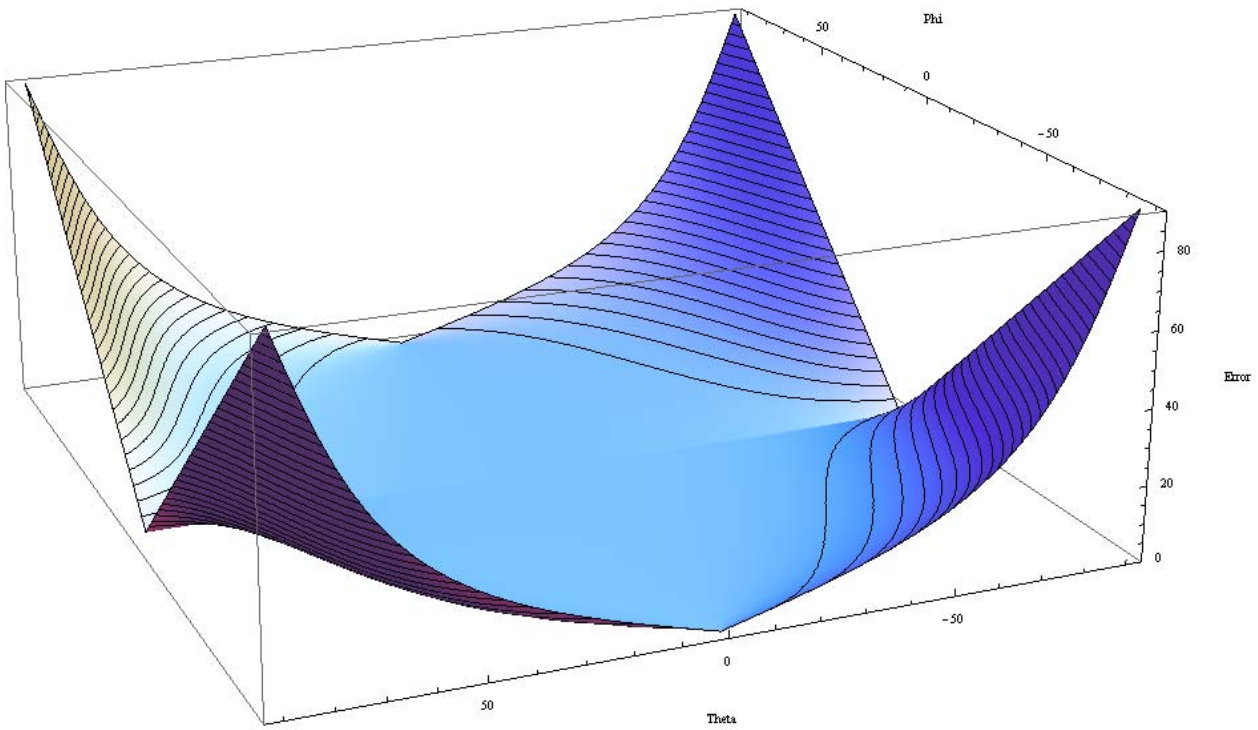

Figure 5. Roll Angle Error Surface $|\Delta\phi|$ for μ = 0.1

A similar strategy can be used for the non-aerospace sequence $\boldsymbol{R}_{yxz}$ to stabilize Equation 29 to give the following equations:

$$\tan\theta_{yxz} = \frac{-G_{px}}{sign(G_{pz})\sqrt{G_{pz}^{2} + \mu G_{py}^{2}}} \qquad \textbf{Eqn. 42}$$

$$\tan\phi_{yxz} = \frac{G_{py}}{\sqrt{G_{px}^{2} + G_{pz}^{2}}} \qquad \textbf{Eqn. 43}$$

The error surface for Equation 42 will have the same form as shown in Figures 4 and 5.

4 Calculating the Angle Between Two Accelerometer Readings

Simple vector algebra provides a means to calculate the angle change α of the apparent gravity vector between any two accelerometer readings.

The scalar product $\boldsymbol{a}.\boldsymbol{b}$ between any two vectors $\boldsymbol{a}$ and $\boldsymbol{b}$ gives the angle α between the two vectors. This result is easily proved by applying the triangle cosine theorem to the triangle with sides comprised of the vectors $\boldsymbol{a}$, $\boldsymbol{b}$ and $\boldsymbol{a}$-$\boldsymbol{b}$.

$$\boldsymbol{a}.\boldsymbol{b} = \begin{pmatrix} a_x \\ a_y \\ a_z \end{pmatrix}.\begin{pmatrix} b_x \\ b_y \\ b_z \end{pmatrix} = a_x b_x + a_y b_y + a_z b_z = |\boldsymbol{a}||\boldsymbol{b}|\cos\alpha \qquad \textbf{Eqn. 44}$$

$$\Rightarrow \cos\alpha = \frac{a_x b_x + a_y b_y + a_z b_z}{\sqrt{a_x^{2} + a_y^{2} + a_z^{2}}\sqrt{b_x^{2} + b_y^{2} + b_z^{2}}} \qquad \textbf{Eqn. 45}$$

The unit vector $\hat{\boldsymbol{n}}$ which is normal to both $\boldsymbol{a}$ and $\boldsymbol{b}$, such that $\boldsymbol{a}$, $\boldsymbol{b}$, and $\hat{\boldsymbol{n}}$ form a right-handed triplet, is given by the vector product:

$$\boldsymbol{a}\times\boldsymbol{b} = \begin{pmatrix} a_x \\ a_y \\ a_z \end{pmatrix}\times\begin{pmatrix} b_x \\ b_y \\ b_z \end{pmatrix} = \begin{vmatrix} \hat{\boldsymbol{i}} & \hat{\boldsymbol{j}} & \hat{\boldsymbol{k}} \\ a_x & a_y & a_z \\ b_x & b_y & b_z \end{vmatrix} = \begin{pmatrix} a_y b_z - a_z b_y \\ a_z b_x - a_x b_z \\ a_x b_y - a_y b_x \end{pmatrix} = |\boldsymbol{a}||\boldsymbol{b}|\hat{\boldsymbol{n}}\sin\alpha \qquad \textbf{Eqn. 46}$$

$$\Rightarrow \hat{\boldsymbol{n}}\sin\alpha = \left(\frac{1}{\sqrt{a_x^{2} + a_y^{2} + a_z^{2}}}\right)\left(\frac{1}{\sqrt{b_x^{2} + b_y^{2} + b_z^{2}}}\right)\begin{pmatrix} a_y b_z - a_z b_y \\ a_z b_x - a_x b_z \\ a_x b_y - a_y b_x \end{pmatrix} \qquad \textbf{Eqn. 47}$$

Figure 6 shows these vector relationships graphically.

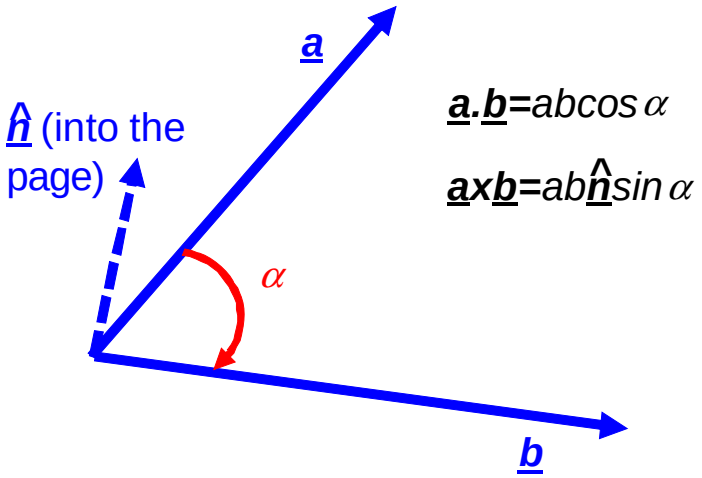

Figure 6. Definitions of the Scalar and Vector Products

Worked Example 2

Two accelerometer readings are recorded (in native units of g) as:

$$\boldsymbol{G}_{p1} = \begin{pmatrix} 0.745439 \\ 0.065434 \\ 0.674523 \end{pmatrix}, \left|\boldsymbol{G}_{p1}\right| = 1.007443 \qquad \textit{Eqn. 48}$$

$$\boldsymbol{G}_{p2} = \begin{pmatrix} 0.393567 \\ 0.348443 \\ 0.844523 \end{pmatrix}, \left|\boldsymbol{G}_{p2}\right| = 0.994750 \qquad \textit{Eqn. 49}$$

Note that as a result of noise or handshake, neither $\boldsymbol{G}_{p1}$ nor $\boldsymbol{G}_{p2}$ have modulus exactly equal to 1g.

Using Equation 45, the angle between the two vectors is:

$$\cos\alpha = \frac{0.745439 \times 0.393567 + 0.065434 \times 0.348443 + 0.674523 \times 0.844523}{1.007443 \times 0.994750} = 0.884606 \Rightarrow \alpha = 27.8° \qquad \textit{Eqn. 50}$$

Using Equation 47, the vector $\hat{\boldsymbol{n}}$ is the instantaneous rotation axis and has direction:

$$\hat{\boldsymbol{n}}\sin\alpha = \left(\frac{1}{1.007443}\right)\left(\frac{1}{0.994750}\right)\begin{pmatrix} a_y b_z - a_z b_y \\ a_z b_x - a_x b_z \\ a_x b_y - a_y b_x \end{pmatrix} = \left(\frac{1}{1.007443}\right)\left(\frac{1}{0.994750}\right)\begin{pmatrix} -0.179772 \\ -0.364070 \\ 0.233990 \end{pmatrix} \qquad \textit{Eqn. 51}$$

$$\Rightarrow \hat{\boldsymbol{n}} = \begin{pmatrix} -0.383610 \\ -0.776878 \\ 0.499304 \end{pmatrix}, \sin\alpha = 0.467626 \Rightarrow \alpha = 27.8° \qquad \textit{Eqn. 52}$$

The vector product calculation confirms the angle of 27.8° between the two gravitational vectors and also provides the vector of the rotation axis $\hat{\boldsymbol{n}}$ normal to the two accelerometer measurements. Direct evaluation proves that the vector $\hat{\boldsymbol{n}}$ is orthogonal to both $\boldsymbol{G}_{p1}$ and $\boldsymbol{G}_{p2}$.

$$\boldsymbol{G}_{p1}.\hat{\boldsymbol{n}} = \begin{pmatrix} 0.745439 \\ 0.065434 \\ 0.674523 \end{pmatrix} \cdot \begin{pmatrix} -0.383610 \\ -0.776878 \\ 0.499304 \end{pmatrix} = 0 \qquad \textit{Eqn. 53}$$

$$\boldsymbol{G}_{p2}.\hat{\boldsymbol{n}} = \begin{pmatrix} 0.393567 \\ 0.348443 \\ 0.844523 \end{pmatrix} \cdot \begin{pmatrix} -0.383610 \\ -0.776878 \\ 0.499304 \end{pmatrix} = 0 \qquad \textit{Eqn. 54}$$

5 Calculating the Tilt Angle

The techniques of the previous section can be used to calculate the angle ρ between the gravitational vector measured by the accelerometer and the initial orientation with the gravitational field pointing downwards along the *z-axis*.

Figure 7. Calculation of the Tilt Angle ρ from Vertical

If the accelerometer reading is $\boldsymbol{G}_p$, then in the absence of linear acceleration:

$$\boldsymbol{G}_p.\begin{pmatrix}0\\0\\1\end{pmatrix} = G_{pz} = \left|\boldsymbol{G}_p\right| cos\rho \Rightarrow cos\rho = \frac{G_{pz}}{\sqrt{G_{px}{}^2 + G_{py}{}^2 + G_{pz}{}^2}} \quad \textit{Eqn. 55}$$

Worked Example 3

The measured accelerometer reading $\boldsymbol{G}_p$ is below. By what angle ρ is the smartphone tilted from its original flat position?

$$\boldsymbol{G}_p = \begin{pmatrix}0.324322\\-0.653423\\0.684234\end{pmatrix} \quad \textit{Eqn. 56}$$

The modulus of $\boldsymbol{G}_p$ is easily determined to be:

$$\sqrt{G_{px}{}^2 + G_{py}{}^2 + G_{pz}{}^2} = 1.000161 \quad \textit{Eqn. 57}$$

Using Equation 55, the tilt angle ρ is:

$$\cos\rho = \frac{0.684234}{1.000161} = 0.684124 \Rightarrow \rho = 46.8° \quad \textit{Eqn. 58}$$

6 Selecting Portrait and Landscape Modes

The first high volume use of accelerometers in consumer products was to switch a display between landscape and portrait orientations. A tablet PC, shown in Figure 8, has four possible display orientations labeled here as Bottom, Top, Right and Left, according to the location of the lower edge of the displayed text or imagery.

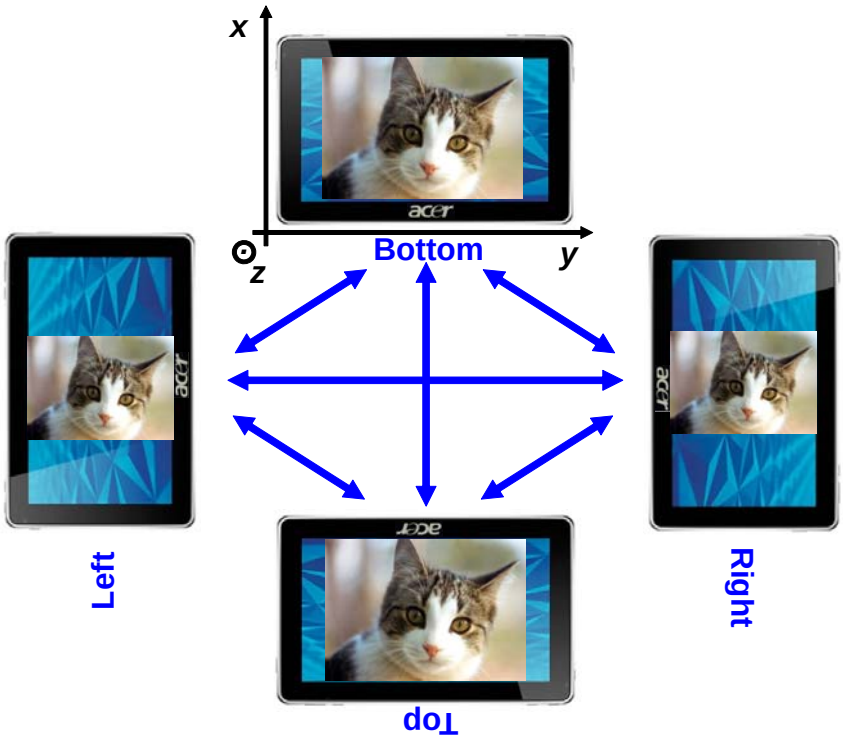

Figure 8. Portrait and Landscape Screen Orientations for a Tablet PC

This problem is rather more complex than it would appear at first sight since a direct mapping between the display orientation and the accelerometer reading is not ergonomically suitable. Specifically, a user viewing the screen in any of the four modes shown in Figure 8 expects that display mode to remain unchanged as the tablet is rotated to a flat orientation. The accelerometer reading resulting from the tablet being flat on the table can therefore be associated with any of the four display orientations.

The solution is a simple state machine in which the accelerometer reading leads to *transitions* between the screen orientations rather than directly defining the screen orientation. Simple state transition rules are listed below.

- ($|G_{pz}| < 0.5g$) AND ($G_{px} > 0.5g$) AND ($|G_{py}| < 0.4g$): Change orientation to Top
- ($|G_{pz}| < 0.5g$) AND ($G_{px} < -0.5g$) AND ($|G_{py}| < 0.4g$): Change orientation to Bottom
- ($|G_{pz}| < 0.5g$) AND ($G_{py} > 0.5g$) AND ($|G_{px}| < 0.4g$): Change orientation to Right
- ($|G_{pz}| < 0.5g$) AND ($G_{py} < -0.5g$) AND ($|G_{px}| < 0.4g$): Change orientation to Left.

The regions in the accelerometer measurement space G_{px}, G_{py}, and G_{pz} corresponding to these rules are shown in Figure 9 with the 1g sphere superimposed.

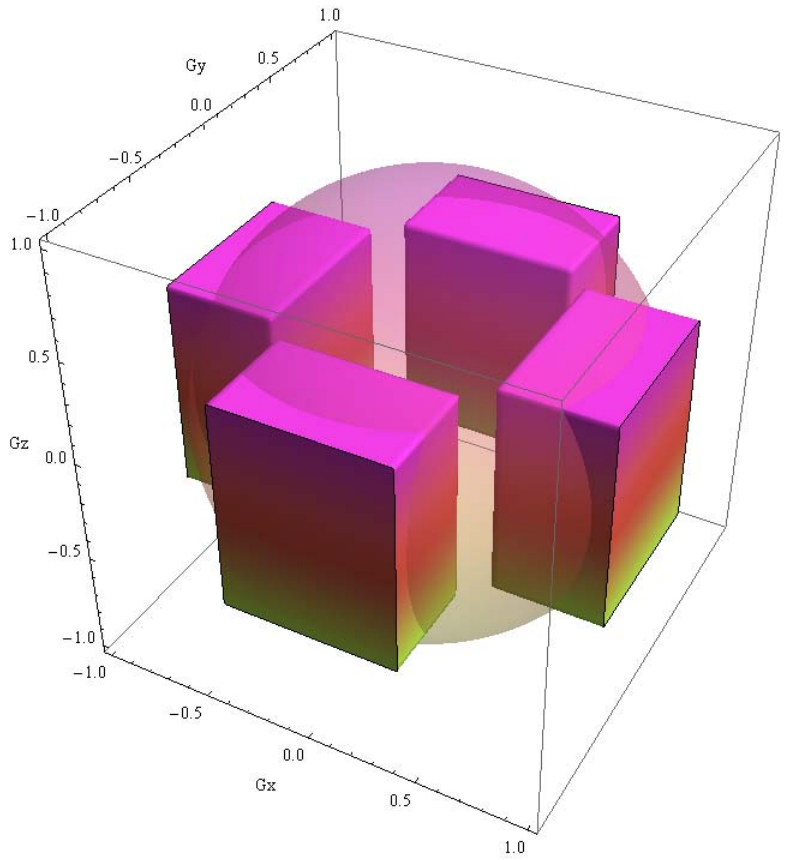

Figure 9. State Transition Zones for Display Orientation Changes

The restriction that $|G_{pz}| < 0.5g$ for a display transition to occur prevents any change in orientation when the tablet is within 0.5g of being complete flat or inverted (since $|G_{pz}| = 1g$ when the tablet is flat). This is known as *z-axis* lockout and ensures that the screen orientation remains unchanged as the user lowers the tablet to a flat orientation.

The remaining constraints define four non-overlapping regions for the transition between the four screen orientations to occur. The lack of overlap between the regions leads to a unique transition within each region and prevents the display orientation oscillating at the boundary between regions.

How to Reach Us:

Home Page:
freescale.com

Web Support:
freescale.com/support

Document Number: AN3461
Rev. 6
03/2013